JACS
JOURNAL OF THE AMERICAN CHEMICAL SOCIETY
Article
pubs.acs.org/JACS

# Peptide Desorption Kinetics from Single Molecule Force Spectroscopy Studies

Stefanie Krysiak,[†,§] Susanne Liese,[‡,§] Roland R. Netz,*[,‡] and Thorsten Hugel*[,†]

[†]Physik Department and IMETUM, Technische Universität München, 85748 Garching, Germany
[‡]Fachbereich für Physik, Freie Universität Berlin, 14195 Berlin, Germany

Supporting Information

**ABSTRACT:** We use a combined experimental/theoretical approach to determine the intrinsic monomeric desorption rate $k_0$ of polytyrosine and polylysine homopeptides from flat surfaces. To this end, single polypeptide molecules are covalently attached to an AFM cantilever tip and desorbed from hydrophobic self-assembled monolayers in two complementary experimental protocols. In the constant-pulling-velocity protocol, the cantilever is moved at finite velocity away from the surface and the distance at which the constant plateau force regime ends and the polymer detaches is recorded. In the waiting-time protocol, the cantilever is held at a fixed distance above the surface and the time until the polymer detaches is recorded. The desorption plateau force is varied between 10 and 90 pN, by systematically changing the aqueous solvent quality via the addition of ethanol or salt. A simultaneous fit of the experimental data from both protocols with simple two-state kinetic polymer theory allows to unambiguously disentangle and determine the model parameters corresponding to polymer contour length $L$, Kuhn length $a$, adsorption free energy $\lambda$, and intrinsic monomeric desorption rate $k_0$. Crucial to our analysis is that a statistically significant number of single-polymer desorption experiments are done with one and the same single polymer molecule for different solvent qualities. The surprisingly low value of about $k_0 \approx 10^5$ Hz points to significant cooperativity in the desorption process of single polymers.

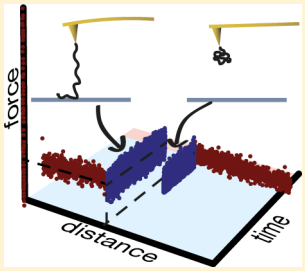


## INTRODUCTION

The desorption kinetics of polymers from solid surfaces is important for a whole range of biological and technological applications. Due to the multiscale nature of the polymer dynamics,[1] the process of polymer desorption from a surface is far more complicated than the desorption of particles with only few internal degrees of freedom, such as molecules, colloids or folded proteins that do not undergo conformational changes upon adsorption. For a simple particle, one expects the desorption rate to decrease exponentially with the adsorption free energy, that is, the higher the surface adhesion, the lower the desorption rate. Adopting the same scaling for polymers, one would accordingly expect the desorption rate to go exponentially down with the polymer length.

In contrast to this naive expectation, the desorption rate for polymers has been experimentally found to scale as an inverse power-law with the monomer number $N$, not exponentially.[2] Initially, this behavior has been associated with the dense adsorption layers that form when polymers adsorb on surfaces from solution.[3] But even for single polymers, power-law scaling for the desorption and adsorption rates has been theoretically found,[4,5] which therefore points to universal power-law desorption dynamics of polymers. This can be rationalized by the dynamic multiscale nature of a polymer, meaning that the polymeric desorption process is independently initiated at different locations by loop formation and occurs simultaneously in a cooperative fashion. This lends much more importance to the exponential prefactor of the rate equation compared to the case of simple particles, where the kinetics is dominated by the exponential factor itself. Single molecule studies are perfectly suited for the experimental study of polymer desorption kinetics and allow to treat the single-polymer case without the additional complications due to multichain effects in dense adsorbed layers.

Over the past two decades various experimental techniques have been introduced which allow to determine the response of single molecules to mechanical force, yielding radically new insight into the mechanisms of intermolecular binding and intramolecular elasticity.[6−9] In a particularly useful setup for the study of polymer−surface interactions, a single, long polymer is firmly (ideally covalently) attached to the tip of an AFM cantilever and the force exerted on the cantilever is measured as a function of the distance from the surface.[10−12] For the case that the polymer adsorbs onto the surface, and depending on the equilibration time of the surface−polymer interactions compared to the experimental time scale, two different scenarios have to be distinguished: If the individual adhesions spots or bonds of the polymer on the surface are very stable and relax slower than the duration of the pulling experiment, a force−distance curve that results from the stretching of the polymer strand connecting the surface and the AFM cantilever is obtained, which basically probes the polymer elasticity. This scenario allows one to study structural force-induced transitions of the polymer chain,[9,13] binding of cosolutes on DNA,[14] and the extension of different polymeric backbones.[15] If, on the

Received: October 7, 2013
Published: December 16, 2013

   dx.doi.org/10.1021/ja410278r | J. Am. Chem. Soc. 2014, 136, 688−697

other hand, the polymer−surface bonds relax faster than the speed with which the cantilever is moved away from the surface, the measured force results from the breaking of polymer−surface bonds and is a measure of the polymer−surface adhesion free energy. In this scenario, which will be the subject of the present study, flat force plateaus are measured that correspond to the quasi-equilibrium desorption of polymers from the surface with negligible influence of the cantilever speed on the recorded forces.

Experimentally, an intermediate situation is also possible, where the polymer gets transiently stuck on the surface as it is moved away and a mixture of polymer stretching and slipping events is recorded in the force−distance curves.[16,17] The crossover between these two limiting scenarios is quantified by the surface mobility of the adsorbed polymer: If this mobility is low compared to the pulling speed, stick events and velocity-dependent forces are expected. If on the other hand mobility is high, flat force plateaus are predicted.[18] Empirically, it is found that, on flat homogeneous surfaces such as polished diamond surfaces[19] or self-assembled monolayers,[20] polymers typically exhibit low surface friction and the force−distance curves display flat force plateaus. Previous work interpreted the desorption plateau force in terms of charge effects,[12,21,22] the hydrophobic effect,[19] surface roughness,[23] and DNA base specificity.[24] In a recent combined experimental/theoretical study, Staple et al.[25] examined the pulling-induced polymer desorption in terms of a two state master equation, under the assumption of detailed balance between the desorption and readsorption processes. While the force plateau value was found to follow from a simple free energy minimization, the plateau lengths, that is, the cantilever distances at which the polymer completely detaches from the surface, were found to strongly depend on the pulling velocity, indicative of the nonequilibrium nature of this process. Interestingly, at typical cantilever velocities in the range of a micrometer per second, polymers were found to detach already when about half of the polymer contour length was still adsorbed on the surface.

In the above-described standard AFM single-polymer desorption experiment, in which the cantilever is continuously moved away from the surface, one measures two quantities, namely, the plateau force and the plateau length. The problem contains four unknowns, namely the polymer contour length, the Kuhn length or persistence length (depending on whether one uses a freely jointed chain or a wormlike chain model), the adsorption free energy per monomer, and the monomeric desorption rate, clearly too many to be unambiguously resolved from a single AFM desorption experiment. In order to obtain the monomeric desorption rate of a single polymer, which experimentally is difficult to measure in standard setups but forms the basis of any theoretical model of adsorption or desorption kinetics, we in this paper perform single-polymer desorption experiments that differ in three aspects from previous approaches:

(1) We perform single-polymer AFM experiments using two complementary protocols, namely, the constant-pulling protocol and the waiting-time protocol. In the constant-pulling protocol, the cantilever is moved away from the surface at constant velocity and the plateau force value and the plateau length are recorded (as in above-described studies). In the waiting-time protocol, the cantilever is moved away from the surface up to a distance at which the polymer is still adsorbed and a nonzero plateau force is measured, then the cantilever distance is held fixed and the time until it detaches from the surface is recorded. The detachment results in a sudden drop of the force to zero. This experiment is repeated for different distances from the surface. By the simultaneous fitting of data in the constant-pulling and waiting-time protocols, we reliably determine all model parameters.

(2) The adsorption free energy and therefore the plateau force is systematically varied by the addition of cosolutes: In our present study we employ two different homopeptides, polytyrosine and polylysine, and a hydrophobic self-assembled monolayer as a substrate. Starting from pure water, where the two homopeptides desorb at around 60−70 pN, we decrease the plateau force values down to 10 pN by the addition of ethanol and increase it up to 90 pN by the addition of salt.

(3) By the very stable covalent binding of the polypeptides to the cantilever tip, we can perform a large number of experiments in the constant-pulling and waiting-time protocols at different solvent conditions with one and the same single polymer. By a simultaneous fit of the resulting data we effectively eliminate one fitting parameter, namely, the contour length, which by construction is the same in such a set of experimental data. By performing such sets of experiments at different solvent conditions with polymer chains of identical monomer type but different chain length, and by again simultaneous fitting the resulting data, we effectively eliminate the Kuhn length (or persistence length) as a fitting parameter. We note that, in one case, we were even able to perform experiments in both constant-pulling and waiting-time protocols and at different solvent conditions with one and the same single polymer and to fit the data consistently with our theoretical model results.

Our theoretical model describes polymer detachment in the constant-pulling and waiting-time protocols using a simple two-state kinetic model. Since reattachment is never observed in the experiments, we only treat the limit of irreversible detachment which allows closed-form solution of the kinetic equations. This means that our kinetic model breaks down at low pulling velocities and short polymers, which however is of no concern for our fitting of the actual experimental data, as we explicitly demonstrate in the Supporting Information. We use the known power-law dependence of the desorption rate $k_0$ on the polymer length, which leaves the intrinsic monomer desorption rate as the only kinetic fitting parameter. The most direct manifestation of the detachment kinetics is possible in the waiting-time protocol, where the theory predicts a steep increase of the waiting time as the cantilever distance from the surface is decreased below the plateau length obtained in the constant-pulling protocol. From the experimental data the intrinsic monomeric desorption rate $k_0$ is determined to be $k_0 = 3.2 \times 10^4$ Hz for polylysine and $k_0 = 3.2 \times 10^5$ Hz for polytyrosine. These surprisingly low values point to considerable cooperativity in the detachment process of single polymers. In the free energetic description of the chain stretching, we compare the semiflexible and the freely jointed chain models, the differences shed light on the model dependence of our results. The plateau length is considerably shorter than the fitted chain contour length, as has been noted before,[25] and the polymers detach via a strongly discontinuous transition. The ratio of plateau length and contour length depends sensitively on the adsorption free energy. Using the derived desorption rate $k_0$ for the description of the constant-pulling protocol experiments, the plateau length for high adsorption energy is predicted to be close to the maximal possible plateau length where only one monomer is still


dx.doi.org/10.1021/ja410278r | J. Am. Chem. Soc. 2014, 136, 688−697

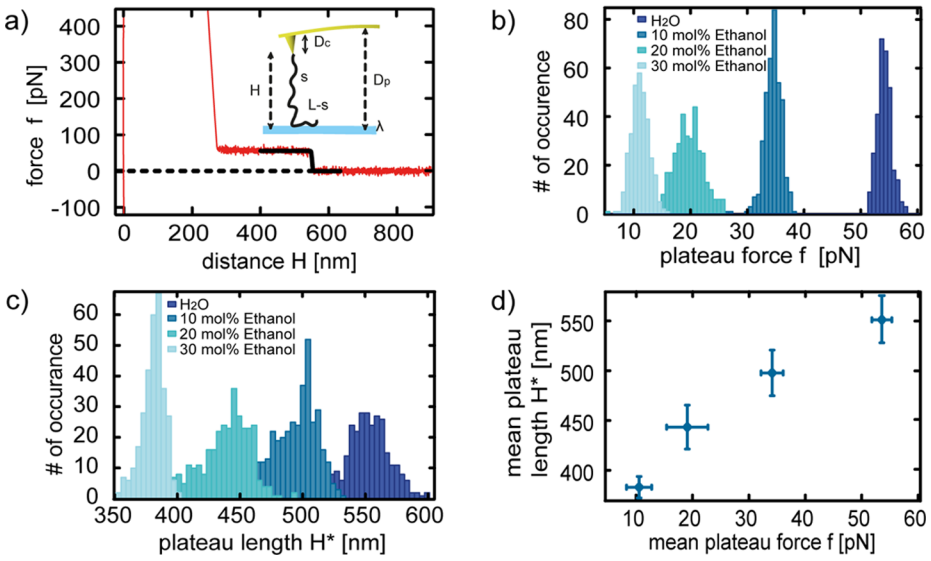


**Figure 1.** Experimental results in the constant-pulling protocol. All experiments are performed with one and the same polylysine chain at a pulling velocity of 1 $\mu$m/s on a hydrophobic SAM. (a) A single force trace in pure water is shown, exhibiting a plateau force of 54 pN and a plateau length of $H^*$ = 550 nm. The inset schematically shows the experimental setup (see main text for details). (b) Plateau force distributions in different water/ethanol mixtures. (c) Plateau length distributions in different water/ethanol mixtures. (d) Plot of the mean plateau length $H^*$ versus the mean plateau force $f$ for the different solvent mixtures shown in (b) and (c). The same data is also included in Figures 4 and 7 and indicated therein as black triangles.

attached to the surface before detachment. The latter finding is relevant for applications of polymers as adhesive bridges between surfaces.[26]

Our paper is organized as follows. First, we display our experimental results in the constant-pulling and waiting-time protocols. Afterward, we first develop the equilibrium theory of AFM-induced polymer desorption and then describe the two-state kinetic model. In the subsequent section, we in detail describe the fitting of the experimental data in the constant-pulling and waiting-time protocols, followed by a brief discussion.

## METHODS

**Surface Preparation.** Glass slides are sonicated for 15 min in a 2% Hellmanex solution (Hellma GMBH, Germany) and twice in ultrapure water (Biochrom, Germany) and then cleaned with RCA solution (v:v:v: 5:1:1 water, 32% ammonia, 35% hydrogen peroxide, VWR, Germany) at 75 °C for 15 min. The slides are coated by a vacuum coater (Edwards GMBH, Kirchheim, Germany) with 10 nm chrom-nickel and 100 nm gold and then stored in the fridge. The gold slides are again cleaned in RCA solution at 75 °C for 15 min and then immersed for 12 h in 2 mM 1-dodecanthiol (Sigma Aldrich, Germany) in ethanol (absolute, >99.9%, Merck, Germany) for the formation of hydrophobic self-assembled monolayers (SAMs). The slides are rinsed with ethanol and ultrapure water before being dried by nitrogen gas. Static contact angle measurements are carried out with a home-built goniometer equipped with a CCD camera and analyzed with Image J drop analysis plugin.[27] We measure contact angles between 105° and 110° for the hydrophobic SAMs. We analyzed the topography of the SAM by AFM and found a root-mean-square (RMS) roughness of 1.7 nm (see Supporting Information Figure S4).

**Tip Functionalization.** Silicon nitride cantilevers (MLCT, Bruker SPM probes, Camarillo, CA) are first activated in an oxygen plasma chamber (Femto, Diener electronic, Germany) for 15 min. Cantilevers are rinsed with dry acetone (VWR, Germany) and then incubated for 10 min in a Vectabond (Axxora, Germany) solution (50 $\mu$L Vectabond in 2.5 mL dry acetone) for silanization. Afterward they are rinsed in dry acetone and dry chloroform (VWR, Germany). A 1:1500 mix of PEG-$\alpha$-$\omega$-Di-NHS (6 kDa, Rapp Polymere GmBH, Tübingen, Germany) and $CH_3O$-PEG-NHS (5 kDa, Rapp Polymere GmBH, Tübingen, Germany) is prepared in dry chloroform, and the cantilevers are incubated for 45 min. The cantilevers are now rinsed in dry chloroform, ethanol, and sodium-borate buffer (50 mM, pH 8.1) and incubated for 1 h in 1 mg/mL polymer solution dissolved in sodium borate buffer. Polymers poly-L-lysine (70−150 kDa) and poly-D-tyrosine (40−100 kDa) are purchased from Sigma Aldrich, Germany. PEG tips are funtionalized following the activation and silanization steps of the protocol above but using only $CH_3O$-PEG-NHS (5 kDa) instead of a PEG mix.

**AFM Measurements.** The measurements are performed with a MFP-3D SA (Asylum Research, Santa Barbara, CA) in a home built fluid cell at room temperature (25 °C). Extension−retraction cycles are measured with a constant pulling velocity of 0.5 or 1 $\mu$m/s and a dwell time on the substrate of 1 s. During the retraction constant force plateaus are observed in the force−distance curves. The plateaus are fitted with sigmoidal curves, and plateau force and plateau length are extracted for each curve. The values of each measurement are plotted in a histogram and fitted with a Gaussian. The maximum of the Gaussian is extracted and the standard deviation is plotted as error. Each polymer on the tip can clearly be distinguished by a distinct peak in the plateau length distribution. This plateau length is different for every tip since our samples are polydisperse. AFM measurements with the PEG modified control cantilevers show no plateaus. For the waiting time measurements, the tip is only partially retracted from the surface and held for a waiting period of 10 or 9.4 s (cutoff time) at fixed tip−surface separation before complete retraction. This is done repeatedly for different distances. The time until detachment is measured. If the desorption occurs after the maximum waiting time, that is, during the final retraction, the cutoff time is used. For each measurement, at least a hundred distance/time pairs are recorded. The software control is programmed based on Igor Pro and Asylums Research's built-in functions. To calibrate the spring constant a thermal noise based procedure is used.[28] The same cantilever is used within one data set. For each solvent the spring constant is measured separately and the averaged value over all measured spring constants for one cantilever is used for the whole data set.

**Fitting Procedure for the Waiting-Time Experiment.** To compare the original experimental waiting-time data $t(H)$ with our model, we average the experimental data for $t(H)$ over finite ranges in $H$ such that at least 10 data points lie in each distance range (cf.


dx.doi.org/10.1021/ja410278r | J. Am. Chem. Soc. 2014, 136, 688−697

Supporting Information for a summary of the original and averaged data). The mean value and the standard deviation of the mean value is calculated for each distance range. Since the experimental waiting-time data exhibit large scattering, it is more robust to fit the integral over the waiting time defined as

$$T(H) = \int_{H_{min}}^{H} \langle t(H') \rangle \, dH' \quad (1)$$

with $\langle t(H') \rangle$ given in eq 15. The lowest pulling distance considered in the experiment is used as lower integration boundary $H_{min}$. The experimental data for $T(H)$ are compared by the least-squares method with the theoretical prediction (which is obtained by numerical integration), and gives $\omega$ and $H_{max}$ (cf. eqs 10 and 15) as fit parameters (see Supporting Information for a summary of all fits).

## RESULTS AND DISCUSSION

**Experiments in the Constant-Pulling and Waiting-Time Protocols.** The inset of Figure 1a shows the schematic setup of the AFM single peptide desorption experiment. A homopeptide of contour length $L$ is terminally attached to the tip of an AFM cantilever. A part of the polymer with the contour length $L - s$ is adsorbed on the solid substrate, in our case a hydrophobic SAM, while the remaining chain section of length $s$ is stretched between the substrate and the cantilever tip located at a distance $H$ above the surface. The adsorbed chain section is subject to an attractive surface potential, which results in the adsorption free energy per unit length $\lambda$ and which creates a force $f$ that is transmitted through the linker polymer section and pulls the cantilever toward the surface. This force is detected via the cantilever deflection of $D_p - D_c - H$, where $D_p$ is the height of the cantilever above the surface in the absence of force and $D_c$ is the size of the cantilever tip. In the pulling protocol, the polymer is pulled at constant velocity away from the surface and the plateau force as well as the plateau length are measured. In Figure 1a, a typical force trace at pulling velocity $v$ = 1 $\mu$m/s for a polylysine chain in pure water is shown. At distances below $H \approx 250$ nm, unspecific forces are recorded, which hide the force plateau of $f$ = 54 pN that is seen at larger distances and extends up to a plateau length of $H^*$ = 550 nm. Figure 1b shows the plateau force distribution in different ethanol/water mixtures, all obtained with the identical single polylysine chain. As can be seen, by adding ethanol, the polymer adsorption free energy to the surface is lowered, resulting in a lower plateau force. This can be rationalized based on the idea that the adsorption on the hydrophobic substrate is due to residual hydrophobic forces between the chain and the surface, which are weakend by the addition of ethanol to the solvent.[29,30] For each solvent mixture, about 300 force traces are recorded; that is, the complete data set in Figure 1b consists of roughly 1000 force traces obtained with one single polylysine chain. Figure 1c shows the distribution of the plateau lengths $H^*$ for the four different solvent mixtures. The typical plateau length goes substantially down as the plateau force decreases, and it is clear that the plateau length for high alcohol contents is substantially smaller than the peptide contour length (which must be larger than the maximal plateau length measured in pure water, here: around 600 nm). Note that the length of different peptide chains used in our experimental study varies substantially, as is common for synthetic polymers, so the data comparison in Figure 1d is meaningful only because all data are recorded with the same individual polypeptide chain, that is, for constant polymer contour length $L$. In Figure 1d, we plot the mean plateau length $H^*$ versus the mean plateau force $f$, which clearly indicates a systematic and pronounced increase of $H^*$ with increasing force.

In the second experimental protocol, the waiting-time protocol, the polymer is pulled up to a certain distance $H$ smaller than the plateau length $H^*$ and the time until the polymer detaches is measured. Figure 2a shows an experimental force trajectory as a function of time and cantilever distance. Figure 2b compares experimental results for a single polytyrosine chain obtained in the two different protocols. The blue bars show the plateau length distribution from experiments in the constant-pulling protocol at a pulling velocity of 1 $\mu$m/s. The plateau lengths are sharply centered around a mean distance of approximately $H^*$ = 155 nm. If the cantilever is held at a fixed position below 155 nm, the polymer detaches after a waiting time that strongly increases as the cantilever distance is reduced, indicated in Figure 2b by red circles. To compare the experimental time scales, we note that pulling the polymer up to a distance of 150 nm only takes 0.15 s, while below a cantilever distance of approximately 110 nm, the waiting time exceeds the maximal waiting time of 10 s in the experiments.

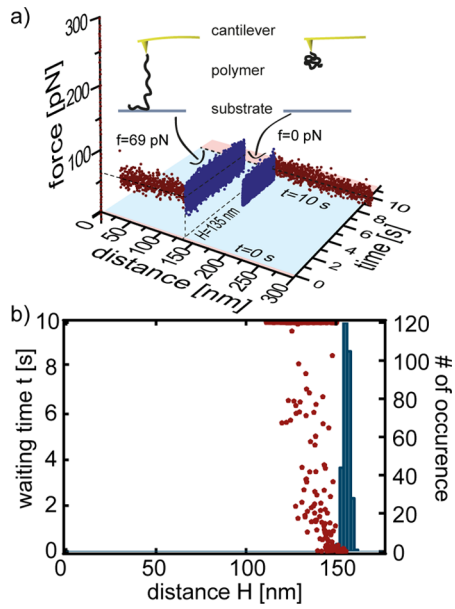


**Figure 2.** Experimental results in the waiting-time protocol: (a) Exemplary force trace as a function of distance from the substrate $H$ and time $t$. First the polytyrosine chain is pulled at a force of $f \approx 69$ pN to a tip−surface separation of $H \approx 135$ nm with a cantilever speed of $v$ = 1 $\mu$m/s. Next the cantilever is held at a fixed position for 10 s. The measured force stays constant for about 4 s and then drops suddenly to zero, which indicates a detachment. After 10 s, the cantilever is retracted from the surface. (b) The results of about 340 waiting-time experiments performed with one identical polytyrosine chain in pure water are indicated by red spheres. The plateau length distribution from the constant-pulling protocol for the same single polytyrosine chain at pulling velocity $v$ = 1 $\mu$m/s is shown in blue, the resulting mean plateau length is $H^*$ = 155 nm. Below $H$ = 110 nm, the waiting time always exceeds the experimental time threshold of 10 s. As the distance approaches the mean plateau length $H^*$, the waiting time approaches zero.

**Theory of Polymer Desorption under Terminal Pulling.** *Equilibrium Plateau Length.* The equilibrium plateau length $H_{eq}$ is determined by the condition that the free energy $F$ of the adsorbed polymer at fixed vertical cantilever position $D_p$


dx.doi.org/10.1021/ja410278r | J. Am. Chem. Soc. 2014, 136, 688−697

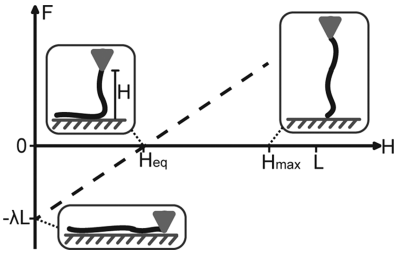


**Figure 3.** Free energy in dependence of the pulling distance $H$. As the pulling distance $H$ increases, the free energy of the system increases linearly (cf. eq 5). At the equilibrium plateau length $H_{eq}$, the stretching free energy of the desorbed chain section equals the adsorption free energy of the adsorbed section and the total free energy crosses zero. If the pulling distance is further increased, the system becomes metastable up to a maximal plateau length $H_{max}$ at which the polymer is adsorbed on the surface only via a single monomer.

equals that of the unperturbed polymer in solution; see the scheme in the inset of Figure 3. The free energy $F$ for a chain of contour length $L$ reads

$$F(s, H, D) = -\lambda(L - s) + \int_0^H f(H'/s)\mathrm{d}H' + \frac{K}{2}(D_p - D_c - H)^2 \quad (2)$$

and consists of three terms accounting for the adsorbed polymer section, the stretched polymer section and the bent cantilever, respectively. The adsorption contribution is given by the product of the adsorption free energy per unit length, $\lambda$, and the contour length of the adsorbed part, $L - s$. The stretching contribution is the integral of the stretching force $f$ of a polymer section of contour length $s$ from the relaxed state at vanishing extension up to the extension $H$. Finally, the cantilever bending energy is proportional to the cantilever stiffness $K$ and the square of the cantilever deformation $D_p - D_c - H$. To estimate the model dependence of our theoretical description, we compare two different models for the chain stretching response. For a freely jointed chain (FJC), the relation between force $f$ and end-to-end distance $H$ is given by[31]

$$\frac{H}{s} = \coth\left(\frac{fa}{k_BT}\right) - \frac{k_BT}{fa} \quad (3)$$

where $a$ is the Kuhn length, $k_B$ is the Boltzmann constant, and $T$ is the absolute temperature. For a wormlike chain (WLC), the interpolation formula from Marko and Siggia is used,[32]

$$\frac{fa}{2k_BT} = \frac{H}{s} + \frac{1}{4(1 - H/s)^2} - \frac{1}{4} \quad (4)$$

where the relation between the effective Kuhn length and the persistence length $l$ is given by $a = 2l$. Note that both force–distance expressions are valid in the large-force limit $fs/(k_BT) > 1$, which is always realized for the experiments we consider (and only in this case the force solely depends on the ratio $H/s$). The equilibrium state for a given cantilever height $D_p$ is obtained by minimizing $F$ with respect to $s$ and $H$, which leads to the two equations

$$\frac{\delta F}{\delta s}|_{s_{min}} = \lambda + \int_0^{H/s_{min}} f(H'/s)\,\mathrm{d}(H'/s) - \frac{H}{s_{min}} f(H/s_{min}) = 0$$

$$\frac{\delta F}{\delta H}|_{H_{min}} = f(H_{min}/s) - K(D_p - D_c - H_{min}) = 0$$

Using these equations, the equilibrium free energy follows as

$$F(s_{min}, H_{min}) = -\lambda L + H_{min} f(H_{min}/s_{min}) + \frac{f(H_{min}/s_{min})^2}{2K} \quad (5)$$

which is schematically depicted in Figure 3. For $H_{min} = 0$, that is, when the polymer is adsorbed on the surface over its entire contour length, the free energy is given by $F = -\lambda L$. For finite tip separation from the surface, the ratio $H_{min}/s_{min}$ and therefore the force $f$ are constant and result in a linear increase of the free energy with increasing $H_{min}$. Since the free energy of the completely detached polymer chain vanishes, the equilibrium plateau length $H_{eq}$ follows from eq 5 by the condition $F = 0$ as

$$\frac{H_{eq}}{L} = \frac{\lambda}{f} - \frac{f}{2KL} \quad (6)$$

In the stiff cantilever limit $KL \gg f$, which in the Supporting Information is shown to be valid for all experimental data considered, the last term becomes irrelevant and we are left with the simple prediction

$$\frac{H_{eq}}{L} = \frac{\lambda}{f} \quad (7)$$

The relation between the adsorption free energy per unit length $\lambda$ and the pulling force $f$ is nontrivial and depends on the polymer model. For the FJC and WLC chain models it is presented in the Supporting Information. Intuitively speaking, the pulling force $f$ is always larger than the adsorption free energy per unit length, $\lambda$, since part of the mechanical pulling work is invested into chain stretching. Hence, eq 7 predicts that the equilibrium plateau length $H_{eq}$ is strictly smaller than the polymer contour length $L$, and the ratio $H_{eq}/L$ approaches 1 for stiff chains (i.e., large Kuhn length $a$) and also, since only the unitless parameter combination $fa/(k_BT)$ appears in the model, for large desorption forces $f$. In Figure 4a and b, we compare experimental data for the plateau length $H^*$ with the prediction for the equilibrium plateau length $H_{eq}$ (broken lines) from eq 7 for six different individual polytyrosine (Y) and polylysine (K) molecules, each molecule denoted by a different symbol. For each molecule, AFM experiments are performed in pure water, in water–ethanol, or in $NaH_2PO_4$ solutions, and each data point presents an average over at least 90 plateaus. We note that different solvent qualities are in our model distinguished only by the value of the adsorption free energy per unit length $\lambda$ and are assumed not to modify the Kuhn length, as should be valid for the relatively high stretching forces considered. As shown before, ethanol decreases the desorption force $f$, on the other hand, addition of $NaH_2PO_4$ to the solvent increases the desorption force (all solvent concentrations and resulting desorption forces are summarized in a table in the Supporting Information). The result in pure water is denoted by a filled symbol and is located toward the upper end of the measured plateau forces. The addition of these two different cosolvents allows us to span a large range of adsorption forces between 10


dx.doi.org/10.1021/ja410278r | J. Am. Chem. Soc. 2014, 136, 688–697

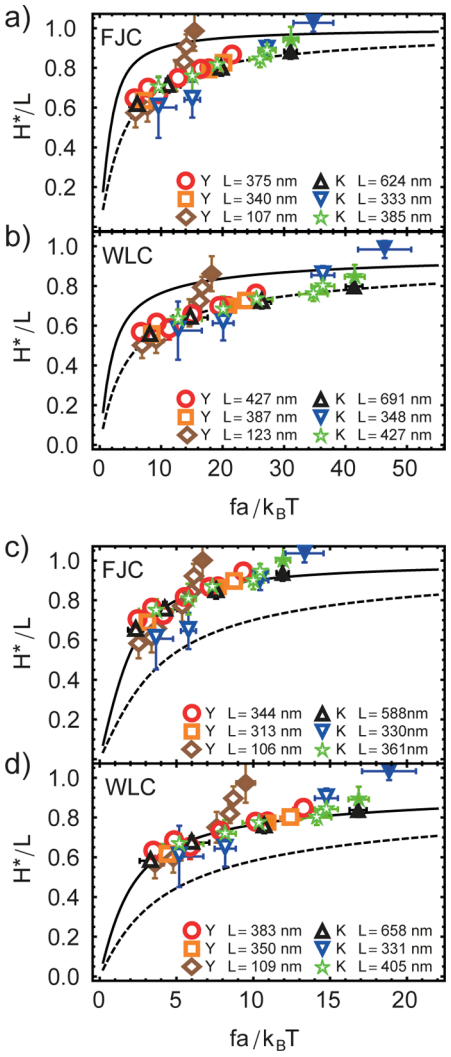


**Figure 4.** Plateau length measurements in the constant-pulling protocol: Three data series for polytyrosine (Y) and three data series for polylysine (K) are shown. Each symbol corresponds to experimental data obtained with one single polymer under different solvent conditions. Measurements in pure water are denoted by filled symbols. The theoretical prediction for the maximal plateau length $H_{max}$ and for the equilibrium plateau length $H_{eq}$ are shown as solid and broken lines, respectively. The fitted contour length of each polymer is given in the subfigures. (a, b) Fit of the experimental plateau length $H^*$ to the theoretical prediction for the equilibrium plateau length $H_{eq}$ of eq 7. (c, d) Fit of the experimental plateau length $H^*$ to the theoretical prediction for the maximal plateau length $H_{max}$ of eq 8.

and 90 pN and thereby to test the theoretical predictions in eq 7 most stringently. The fitted contour length $L$ for each polymer is given in the figures, the Kuhn length is assumed not to depend on the solvent condition and we obtain $a_{Tyr} = 0.99 \pm 0.02$ nm, $a_{Lys} = 2.4 \pm 0.3$ nm for the FJC model and $a_{Tyr} = 1.17 \pm 0.02$ nm, $a_{Lys} = 3.2 \pm 0.5$ nm for the WLC model. By plotting the data as $H^*/L$ versus $fa/(k_BT)$, the prediction for $H_{eq}$ from eq 7 presents a universal curve. Note that, in order not to cluster the figure, we present the data fits for the FJC and WLC models in separate figures. The fact that contour and Kuhn lengths come out differently when using different chain models has been noted and discussed before[33] and is of no concern for our present study. The main conclusion from Figure 4a and b is that the equilibrium plateau length $H_{eq}$ from eq 7 gives a good global description of the plateau lengths for different polymer contour lengths and desorption forces. The data follow a universal curve that for the highest desorption forces obtained in our experiments predicts the plateau length to reach about 80% of the contour length; for the lowest plateau forces of about 10 pN, the plateau length becomes as low as 50% of the contour length. This conclusion is independent of the chain model used (FJC versus WLC) and therefore fairly robust. However, in hindsight of the kinetic model discussed later, we note that the desorption process in fact is not in equilibrium, such that the fitting values obtained for $L$ and $a$ in Figure 4 can at best be viewed as effective parameters. Interestingly, the experimental data for the plateau length in the constant-pulling protocol shown in Figure 4 do not reveal that $H_{eq}$ is not a very realistic estimate for the experimental desorption length, which can only be realized by comparing waiting time with constant-pulling protocol measurements.

*Maximal Plateau Length.* When the cantilever reaches the equilibrium separation $H_{eq}$, a finite number of monomers $(L - s)/a$ is still adsorbed on the substrate. We do not precisely know via which kinetic pathway the desorption transition at a fixed cantilever distance $H$ proceeds, but it is clear that a pronounced free energy barrier has to be overcome. It is therefore plausible that, depending on the pulling speed, the chain will stay adsorbed on the surface in a metastable state even for $H > H_{eq}$. Figure 3 shows the minimized free energy landscape $F$ of eq 5 as a function of the cantilever tip position $H$. The equilibrium desorption transition is defined by $F = 0$ and occurs at the equilibrium plateau length $H_{eq}$, but the graph shows that a metastable state exists up to a maximal plateau length $H_{max}$ at which the polymer is connected to the surface only via a single adsorbed monomer. Depending on the pulling speed, and assuming that the desorbed contour length $s$ is a state variable that rather quickly equilibrates, the polymer might follow this metastable free energy branch up to a certain distance so that the actual desorption transition occurs at a certain cantilever distance between $H_{eq}$ and $H_{max}$. This maximal plateau length $H_{max}$ for a given pulling force $f$ is thus obtained by setting the desorbed polymer contour length $s$ equal to the total polymer contour length $L$. According to eqs 3 and 4, the ratio $H_{max}/L$ follows directly as

$$\frac{H_{max}}{L} = \coth\left[\frac{fa}{k_BT}\right] - \frac{k_BT}{fa}\ (\text{FJC}) \quad \text{and}$$

$$\frac{fa}{k_BT} = 2\left[\frac{H_{max}}{L} + \frac{1}{4(1 - H_{max}/L)^2} - \frac{1}{4}\right]\ (\text{WLC}) \tag{8}$$

Figure 5 compares the equilibrium and maximal plateau lengths $H_{eq}$ and $H_{max}$ for the FJC and WLC models. Both $H_{max}$ and $H_{eq}$ approach the contour length for large forces. In Figure 4c and d, the plateau length results for three polytyrosine and three polylysine chains are fitted using the theoretical prediction for the maximal plateau length $H_{max}$. The fitted Kuhn lengths are $a_{Tyr} = 0.43 \pm 0.02$ nm, $a_{Lys} = 0.92 \pm 0.08$ nm for the FJC and $a_{Tyr} = 0.61 \pm 0.04$ nm, $a_{Lys} = 1.3 \pm 0.1$ nm for the WLC model. Both chain models show similar behavior. $H_{max}$ is strictly larger than $H_{eq}$ but still considerably smaller than the contour length $L$. The fits are of similar quality as the ones in Figure 4a and b using the equilibrium prediction $H_{eq}$, the only difference is that the obtained Kuhn lengths are considerably smaller. One realizes that, based on plateau length


dx.doi.org/10.1021/ja410278r | J. Am. Chem. Soc. 2014, 136, 688−697

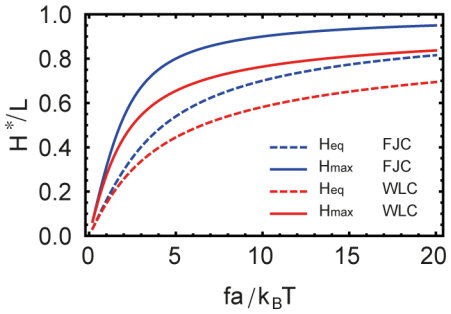


**Figure 5.** Equilibrium plateau length $H_{eq}$ from eq 7 (dashed lines) and maximal plateau length $H_{max}$ from eq 8 (continuous lines) as a function of the pulling force $f$. Blue curves represent results using the FJC model, and red curves correspond to the WLC model.

measurements in the constant-pulling protocol alone, it is not clear whether the desorption process occurs in equilibrium. Based on experiments in the waiting-time protocol, we will below see that for the longer chains $H_{max}$ gives in fact a much better description of the actual plateau lengths.

*Desorption Kinetics.* A polymer of finite contour length adsorbed to a surface will detach within a finite time span because of the translational entropy gain in the detached state, regardless of how strong the adhesive surface potential is. Experimental and theoretical works have shown that the desorption time obeys a power-law in dependence of the polymer length[2−4] and thus deviates fundamentally from an ordinary Arrhenius law that would predict an exponential dependence on the adsorption free energy which scales linearly in polymer length. In the Supporting Information, we demonstrate that an exponential dependence of the desorption rate on the polymer length cannot describe our data and therefore can be generally ruled out. A simple scaling prediction for the desorption kinetics of a polymer chain starts from the scaling of the unperturbed chain radius $R$ as $R \sim aN_{ads}^{\nu}$, where $N_{ads} \sim (L - s)/a$ is the number of adsorbed monomers. The chain desorption is not governed by a single reaction coordinate, for example, the center of mass position, and therefore, there is no reason why the desorption rate should scale exponentially in $N_{ads}$. Rather, the chain desorption proceeds simultaneously via the activated motion of all monomers in parallel. Therefore, the diffusivity of the chain center-of-mass position governing the desorption kinetics can be written as $D \sim a^2 k_0 \, e^{-\lambda a/k_B T}/N_{ads}$, where the prefactor $k_0$ is the effective desorption rate of a monomer that takes into account the effects of cooperativity due to the connectivity between neighboring monomers. Note that we assume the diffusivity to exponentially depend on the adsorption free energy of a single monomer, $\lambda a$, we therefore neglect the possible influence of the adsorption energy on the cooperativity which would amount to an $N$-independent factor in the exponent. We also assume free draining conditions and neglect any hydrodynamic effects as should be justified close to the wall. The time for the chain to diffuse a distance $R$ away from the surface is $\tau \sim R^2/D$, so we conclude the desorption rate $k \sim 1/\tau$ to be given by $k = k_0 \, e^{-\lambda a/(k_B T)}/N_{ads}^{-2\nu-1}$. Since for a force plateau the ratio of the fraction of desorbed chain contour length $s$ and the chain stretching $H$ is constant, $H/s = H_{max}/L$, we have $N_{ads} = (L - s)/a = N(1 - s/L) = N(1 - H/H_{max})$. We thus find

$$k = \frac{\omega}{(H_{max} - H)^{2\nu+1}} \tag{9}$$

where we have defined the effective diffusivity parameter

$$\omega = k_0 \, e^{-\lambda a/k_B T} \frac{H_{max}^{2\nu+1}}{(L/a)^{2\nu+1}} \tag{10}$$

and used $N = L/a$. In the actual data fitting, we will use the Gaussian exponent $\nu = 1/2$ for simplicity.

*Nonequilibrium Effects in the Constant-Pulling Protocol.* The actual plateau length $H^*$ will be smaller than the maximal plateau length $H_{max}$ derived in eq 8, realized for infinitely fast pulling, and larger than the equilibrium plateau length $H_{eq}$ derived in eq 7. We note that in our kinetic description we assume that the variable $s$, which measures the contour length of the desorbed polymer strand, relaxes quickly and is always in local equilibrium. This is accurate if the surface friction of the adsorbed polymer strand is negligible and also means that the desorbed polymer strand is oriented vertically to the adsorbing surface and flat force plateaus are expected, see the detailed discussion of the mechanical force equilibrium conditions in ref 34. As an additional approximation, we treat the polymer desorption process as irreversible, which reflects the experimental fact that reattachment of a detached polymer is not observed for sufficiently large tip−surface separation. The advantage of this approximation is that the kinetic equations can be solved in closed form, which simplifies the fitting of experimental data considerably. In the Supporting Information, we compare this irreversibility approximation with a calculation that allows for reattachment and see that for our experimental parameters reattachment is indeed negligible. Hence, we model the probability of the polymer to be adsorbed, $P_{ads}$, by the first order rate equation that only allows for chain desorption,

$$\frac{dP_{ads}}{dt} = -k(H)P_{ads} \tag{11}$$

Inserting for the desorption rate $k(H)$ the explicit expression in eq 9 and utilizing that in the constant-pulling protocol we have $v = dH(t)/dt$, the rate equation can be integrated exactly and the probability $P_{ads}$ results as

$$\begin{aligned} P_{ads}(H(t)) &= \exp\left[-\int_0^{H(t)} \frac{k(H')}{v} \, dH'\right] \\ &= \exp\left[-\frac{\omega}{vH_{max}(H_{max}/H(t) - 1)}\right] \end{aligned} \tag{12}$$

which fulfills the condition that at time $t = 0$, or equivalently at $H = 0$, the polymer is adsorbed and therefore $P_{ads}(H = 0) = 1$. Defining the probability to be detached as $P_{des} = 1 - P_{ads}$, the probability density to detach at a certain distance $H$, $p_{des} = dP_{des}/dH$, can be used to calculate the mean plateau length $\langle H^* \rangle$ as

$$\begin{aligned} \langle H^* \rangle &= \int_0^{H_{max}} H p_{des} \, dH \\ &= H_{max}\left(1 + \frac{\omega}{vH_{max}} \, e^{\omega/vH_{max}} Ei\left(-\frac{\omega}{vH_{max}}\right)\right) \end{aligned} \tag{13}$$

where the exponential integral $Ei$ has been used. For small absolute values of the argument $\omega/(vH_{max}) = k_0 H_{max} \, e^{(-\lambda a)/(k_B T)}/(vN^2)$, the exponential integral only grows logarith-


dx.doi.org/10.1021/ja410278r | J. Am. Chem. Soc. 2014, 136, 688−697

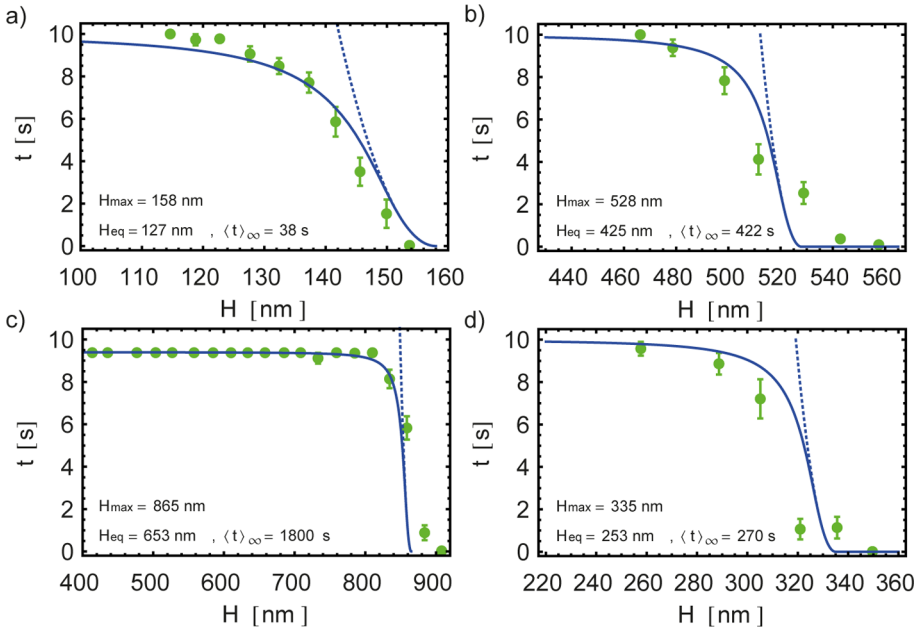


**Figure 6.** Waiting-time measurements for two polytyrosine chains (a, b) and two polylysine chains (c, d) in pure water. In (a), (b), and (d), the upper time cutoff is $t^* = 10$ s; in (c), the upper time cutoff is $t^* = 9.4$ s. The fitted diffusivity parameters are $\omega = 23.81$ nm$^2$/s (a), 24.70 nm$^2$/s (b), 25.60 nm$^2$/s (c), and 26.65 nm$^2$/s (d). The mean waiting-time data together with the standard deviation of the mean value are shown as green data points, while blue solid lines show the fitted theoretical curve. The broken line shows the theoretical curve expected for infinite time cutoff $t^* = \infty$. In each subfigure the equilibrium plateau length $H_{eq}$ (for a FJC model) is given as well as the waiting time $\langle t\rangle_\infty$ at this position assuming an infinite time cutoff. Note that, in each subfigure, all data are obtained with a single identical polypeptide molecule. With the same single polylysine chain that is used in (d) also plateau length measurements in the constant-pulling protocol were performed (blue down triangle in Figures 4 and 7).

mically, $Ei(-\omega/(vH_{max})) \simeq \ln(\omega/(vH_{max}))$, so that the deviation of $\langle H^*\rangle$ from $H_{max}$ to leading order is linear in $\omega/(vH_{max})$; in other words, for fast pulling velocity $v$, high polymerization index $N$, and large adsorption energies $\lambda a/k_BT \gg 1$, the mean plateau length is close to the maximal plateau length. On the other hand, for weakly adsorbing surfaces, for slow pulling, and for short polymers, the desorption process will approach equilibrium (and the irreversible approximation we have used will break down; see the Supporting Information).

*Nonequilibrium Effects in the Waiting-Time Protocol.* In the waiting-time protocol, the cantilever is held at a fixed tip−surface separation $H$ and the time until the polymer detaches is measured. Since in the actual experiment the polymer is pulled at constant velocity $v$ up to a distance $H$, the initial adsorption probability is $P^{wt}_{ads}(t = 0) = P_{ads}(H)$ with $P_{ads}(H)$ given in eq 12, where the superscript wt refers to the waiting-time protocol. The probability $p^{wt}_{des}(t)$ to detach at a certain time $t$ follows from the linear rate equation and is a simple exponential in time

$$p^{wt}_{des}(t) = \frac{d(1 - P^{wt}_{ads}(t))}{dt} = P_{ads}(H)\, k(H)\, e^{-k(H)t} \tag{14}$$

To compare the mean waiting time $\langle t\rangle$ with experimental data we introduce the upper time cutoff $t^*$ which in experiments is typically set to $t^* = 10$s,

$$\begin{aligned}\langle t\rangle &= \int_0^{t*} t p^{wt}_{des}(t)\, dt + \int_{t*}^{\infty} t^* p^{wt}_{des}(t)\, dt \\ &= P_{ads}(H)\frac{1 - e^{-k(H)t*}}{k(H)} \\ &= e^{-\omega H/H_{max}(H_{max}-H)v}\left(\frac{1 - \exp\left[\frac{-\omega t^*}{(H_{max}-H)^2}\right]}{\frac{\omega}{(H_{max}-H)^2}}\right)\end{aligned} \tag{15}$$

In the limit of an infinite time cutoff $t^* \to \infty$ the mean waiting time simplifies to

$$\begin{aligned}\langle t\rangle_\infty &= \int_0^{\infty} t p^{wt}_{des}(t) dt \\ &= \frac{P_{ads}(H, v)}{k(H)} \\ &= e^{-\omega H/H_{max}(H_{max}-H)v}\frac{(H_{max} - H)^2}{\omega}\end{aligned} \tag{16}$$

When comparing eq 15 with experimental waiting-time data, it is important to realize that only the two composite parameters $H_{max}$ and $\omega$ appear as free fitting parameters. The underlying physical parameters $\lambda$, $k_0$, $L$, and $a$ can be obtained by additionally fitting the plateau length data in the constant-pulling protocol, as will be explained in the next section.

**Kinetic Fit of Experimental Data.** *Waiting-Time Protocol.* The waiting-time experiments are performed with two polylysine and two polytyrosine chains in pure water with a time cutoff of $t^* = 10$ or 9.4 s. The averaged experimental data for the four different single polymers chains (green data points) together with the theoretical fits (blue line) according to eq 15 are shown in Figure 6. In all fits, a diffusivity parameter of about


dx.doi.org/10.1021/ja410278r | J. Am. Chem. Soc. 2014, 136, 688−697

$\omega \approx 25$ nm$^2$/s is obtained (see caption for the individual fit values). The fitted maximal plateau length values $H_{max}$ are quoted in the subfigures. The fitting procedure is explained in the Methods section. Figure 6 also shows the mean desorption time expected for an infinite time cutoff given in eq 16 (dotted line), which diverges quickly as $H$ is decreasing. The range in $H$ over which the mean waiting time interpolates between the cutoff $t^*$ and zero has a thickness of 50−100 nm, largely independent of the absolute contour length of the polymer. This indicates that the adsorbed polymer contour length rather then the total polymer contour length determines the mean waiting time. This directly follows from eq 15 which depends on the distance $H_{max} - H$ and on the ratio $H_{max}/L$ but not on the contour length $L$ itself.

*Constant-Pulling Protocol.* For a fit of the plateau length data in the constant-pulling protocol, that were shown already in Figure 4, using the nonequilibrium prediction in eq 13, we use the value $\omega = 25$ nm$^2$/s from the waiting-time data as explained above. This allows us to express $k_0$ as a function of $\lambda$, $L$, and $a$ (see eq 10). Noting in addition that the plateau force $f$ is measured during the experiment, from which the adsorption free energy per unit length, $\lambda$, can be derived (see the Supporting Information), the number of free physical parameters $\lambda$, $k_0$, $L$, and $a$ is reduced to two, namely, the Kuhn length $a$ and the polymer contour length $L$. The fits are shown in Figure 7 as a function of the rescaled plateau length $H^*/L$ and the dimensionless plateau force $fa/(k_BT)$ and are denoted by colored broken lines; each line stands for one individual polymer and corresponds to a series of different solvent conditions. The theoretical predictions for the maximal plateau length $H_{max}$ from eq 8 and the equilibrium plateau length $H_{eq}$ from eq 7 are shown as solid and broken lines, respectively. The kinetic fits according to eq 13 typically lie between the two estimates and for the shortest polymer at the smallest plateau forces actually fall below the curve for $H_{eq}$, which signals a breakdown of our assumption of irreversible adsorption (for an in-depth discussion of the effects of reattachment, see the Supporting Information). We again contrast results for the FJC and WLC models. In the fits, we use the same Kuhn length for all different solvent conditions and obtain the values $a_{Tyr} = 0.73 \pm 0.02$ nm, $a_{Lys} = 0.63 \pm 0.08$ nm for the FJC and $a_{Tyr} = 0.77 \pm 0.02$ nm, $a_{Lys} = 0.69 \pm 0.09$ nm for the WLC model. Both WLC and FJC models describe the data equally well and give quite similar values for the Kuhn length. The values are in good agreement with theoretical estimates based on more refined freely rotating chain models[35] and with experimental WLC fits on stretching curves for these samples on gold (data not shown). Note that the Kuhn length for the identical chemical species agrees much better than that for the fits in Figure 4, which shows that the kinetic model is more realistic. The polylysine chains, used in our experiments, are on average longer than the polytyrosine chains. Hence, the plateau length of polylysine is close to the maximal plateau length. Comparing the Kuhn lengths for polylysine from Figures 4 and 7, a fit to the maximal plateau length gives a better estimate of the Kuhn length obtained in the kinetic fit than a fit to the equilibrium plateau length. Polytyrosine in contrast exhibits larger deviation from the maximal desorption length, and also the Kuhn lengths lie between values obtained in Figure 4. With the Kuhn lengths obtained above, a typical pulling force in water of $f = 70$ pN for polytyrosine, $f = 60$ pN for polylysine, and $\omega = 25$ nm$^2$/s from the waiting-time experiment, the intrinsic desorption rate follows as $k_0 = 10^{5.5\pm0.3}$ Hz $\approx 3.2 \times 10^5$ Hz for polytyrosine and $k_0 = 10^{4.5\pm0.2}$ Hz $\approx 3.2 \times 10^4$ Hz for polylysine, which constitute the main results of our analysis. A comparison with the maximal plateau length (reproduced as black solid line in Figure 7) shows that the nonequilibrium fit in Figure 7 gives a nonequilibrium plateau length that is quite close to the maximal plateau length $H_{max}$, particularly for long polymers and large pulling force. In pure water the ratio $H^*/L$ lies between 80% and 90% for the FJC and between 70% and 80% for the WLC model. The shorter the polymer and the smaller the pulling force, the more pronounced is the deviation from the maximal plateau length. From the obtained fit parameters, the equilibrium adsorption length $H_{eq}$ as well as the mean waiting time $\langle t \rangle_\infty$ for a cantilever held at $H_{eq}$ is given in each subfigure in Figure 6 (note that in this calculation we used the FJC model). Depending on the contour length of the polymer, the mean waiting time at the equilibrium plateau length $H_{eq}$ ranges from several seconds up to half an hour. This drastically demonstrates how far from equilibrium these single molecule experiments are even for relatively short polymers.

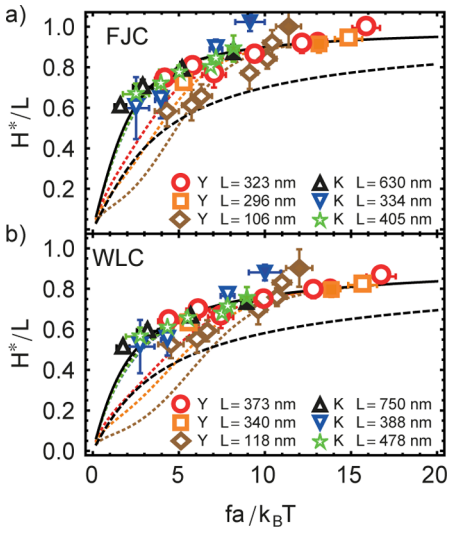


**Figure 7.** Scaling plot of the rescaled experimental plateau length $H^*/L$ versus the rescaled plateau force $fa/(k_BT)$ for six different single polypeptide chains (three polytyrosine (Y) and three polylysine (K) chains) obtained in the constant-pulling protocol. For each single chain, denoted by a different symbol, experiments in a series of different solvent mixtures were performed and the contour length $L$ (quoted in the subfigures) and Kuhn lengths $a$ were obtained from a fit to eq 13. The fit functions are denoted by colored dotted lines. The continuous black line indicates the maximal plateau length $H_{max}$ from eq 8, and the dashed black line the equilibrium plateau length $H_{eq}$ from eq 7. The data indicated by the blue down triangle was obtained with the identical single polymer as the waiting-time experiment shown in Figure 6d.

## CONCLUSION

The force-induced desorption of single polypeptide chains from a solid surface is studied using single-molecule force spectroscopy. By performing experiments with identical single chains in a series of different solvents and in two different experimental protocols, the constant-pulling and the waiting-time protocols, the comparison with a simple two-state kinetic desorption model allows to extract not only the equilibrium chain parameters corresponding to the Kuhn length $a$, contour length $L$, and adsorption free energy per unit length $\lambda$, but also


dx.doi.org/10.1021/ja410278r | J. Am. Chem. Soc. 2014, 136, 688−697

the effective single-monomer desorption rate $k_0$. This rate is found to have the value of about $k_0 \approx 10^5$ Hz and thus is much smaller than the relaxation rate of a single monomer which is of the order of $10^{10}$ Hz.[36] We conclude that the chain connectivity, that is, the fact that each monomer is part of a polymer and thereby configurationally coupled to its neighbors, leads to hindered kinetics and thus to the enormous slow-down by 5 orders of magnitude. This has important consequences for the kinetics of protein folding and all other processes where peptide chains reconfigure in a bound state. We also find that the plateau length at which the polymer detaches from the surface is considerably smaller than the contour length and is given by a universal curve (which differs slightly when comparing FJC and WLC models) that depends sensitively on the adsorption force. At finite pulling velocity, the actual plateau length lies between the equilibrium prediction (realized at vanishing pulling velocity) and the maximal plateau length where only a single monomer is attached to the surface. For long polymers or fast pulling, the maximal plateau length describes the nonequilibrium desorption process quite well, for short polymers or slow pulling the equilibrium prediction becomes accurate. The Kuhn length that we extract from our kinetic model differs only slightly between the FJC and WLC models and for polylysine as well as polytyrosine is about 50% larger than the distance between neighboring $C_\alpha$ atoms. Our model uses a power-law dependence of the desorption rate on the polymer length, based on previous experimental and theoretical results.[2,4] In our analysis, we used a simplified irreversible detachment description that neglects reattachment of a detached chain to the surface at separations where the detachment process occurs, in line with the fact that reattachment was never observed in the experiments. In the Supporting Information, we show that much smaller pulling velocities of 0.01 $\mu$m/s are needed in order to obtain reattachment in the constant-pulling protocols. Future AFM experiments should probe this interesting regime in more depth.

## ■ ASSOCIATED CONTENT

### Supporting Information

Further discussions of an exponentially increasing desorption rate, the reversible desorption and surface characterization. This material is available free of charge via the Internet at http://pubs.acs.org.

## ■ AUTHOR INFORMATION


### Corresponding Authors

rnetz@physik.fu-berlin.de
thugel@mytum.de

### Author Contributions

[§]S.K. and S.L. contributed equally.


### Notes

The authors declare no competing financial interest.

## ■ ACKNOWLEDGMENTS

Helpful discussions with R. Bruinsma, H. J. Kreuzer, and B. N. Balzer are acknowledged. We acknowledge financial support form the DFG Collaborative Research Center SFB 765 (to R.R.N.) and SFB 863 (to T.H.). S.K. was supported by the Elitenetzwerk Bayern in the framework of the doctorate program Material Science of Complex Interfaces.

## ■ REFERENCES


(1) de Gennes, P. G. *Scaling Concepts in Polymer Physics*; Cornell University Press: Ithaca, NY, 1979.
(2) Johnson, H. E.; Douglas, J. F.; Granick, S. *Phys. Rev. Lett.* **1993**, *70*, 3267−3270.
(3) de Gennes, P. G. *Adv. Colloid Interface Sci.* **1987**, *27*, 189−209.
(4) Wang, Y.; Rajagopala, R.; Mattice, W. L. *Phys. Rev. Lett.* **1995**, *74*, 2503−2506.
(5) Descas, R.; Sommer, J. U.; Blumen, A. *J. Chem. Phys.* **2006**, *124*, 094701-8.
(6) Smith, S. B.; Finzi, L.; Bustamante, C. *Science* **1992**, *258*, 1122−1126.
(7) Florin, E. L.; Moy, V. T.; Gaub, H. E. *Science* **1994**, *264*, 415−417.
(8) Cluzel, P.; Lebrun, A.; Heller, C.; Lavery, R.; Viovy, J.; Chatenay, D.; Caron, F. *Science* **1996**, *271*, 792−794.
(9) Rief, M.; Gautel, M.; Oesterhelt, F.; Fernandez, J. M.; Gaub, H. E. *Science* **1997**, *276*, 1109−1112.
(10) Senden, T.; di Meglio, J.-M.; Auroy, P. *Eur. Phys. J. B* **1998**, *3*, 211−216.
(11) Chatellier, X.; Senden, T. J.; Joanny, J.-F.; di Meglio, J.-M. *Europhys. Lett.* **1998**, *41*, 303−308.
(12) Hugel, T.; Seitz, M. *Macromol. Rapid Commun.* **2001**, *22*, 989−1016.
(13) Neuert, G.; Hugel, T.; Netz, R. R.; Gaub, H. E. *Macromolecules* **2006**, *39*, 789−797.
(14) Krautbauer, R.; Clausen-Schaumann, H.; Gaub, H. E. *Angew. Chem.* **2000**, *39*, 3912−3915.
(15) Hugel, T.; Rief, M.; Seitz, M.; Gaub, H. E.; Netz, R. R. *Phys. Rev. Lett.* **2005**, *94*, 048301.
(16) Kuehner, F.; Erdmann, M.; Sonnenberg, L.; Serr, A.; Morfill, J.; Gaub, H. E. *Langmuir* **2006**, *22*, 11180−11186.
(17) Balzer, B. N.; Gallei, M.; Hauf, M. V.; Stallhofer, M.; Wiegleb, L.; Holleitner, A.; Rehahn, M.; Hugel, T. *Angew. Chem., Int. Ed. Engl.* **2013**, *52*, 6541−6544.
(18) Serr, A.; Netz, R. R. *Europhys. Lett.* **2006**, *73*, 292−298.
(19) Horinek, D.; Serr, A.; Geisler, M.; Pirzer, T.; Slotta, U.; Lud, S. Q.; Garrido, J. A.; Scheibel, T.; Hugel, T.; Netz, R. R. *Proc. Natl. Acad. Sci. U.S.A.* **2008**, *105*, 2842−2847.
(20) Schwierz, N.; Horinek, D.; Liese, S.; Pirzer, T.; Balzer, B. N.; Hugel, T.; Netz, R. R. *J. Am. Chem. Soc.* **2012**, *134*, 19628−19638.
(21) Friedsam, C.; Gaub, H. E.; Netz, R. R. *Europhys. Lett.* **2005**, *72*, 844−850.
(22) Pirzer, T.; Geisler, M.; Hugel, T. *Phys. Biol.* **2009**, *6*, 025004.
(23) Geisler, M.; Horinek, D.; Hugel, T. *Macromolecules* **2009**, *42*, 9338−9343.
(24) Manohar, S.; Mantz, A. R.; Bancroft, K. E.; Hui, C.; Jagota, A.; Vezenov, D. V. *Nano Lett.* **2008**, *8*, 4365−4372.
(25) Staple, D. B.; Geisler, M.; Hugel, T.; Kreplak, L.; Kreuzer, H. J. *New J. Phys.* **2011**, *13*, 013025.
(26) Moreira, A. G.; Marques, C. M. *J. Chem. Phys.* **2004**, *120*, 6229−6237.
(27) Stalder, A. F.; Kulik, G.; Sage, D.; Barbieri, L.; Hoffmann, P. *Colloids Surf., A* **2006**, *286*, 92−103.
(28) Pirzer, T.; Hugel, T. *Rev. Sci. Instrum.* **2009**, *80*, 035110−1−035110−6.
(29) Pirzer, T.; Hugel, T. *ChemPhysChem* **2009**, *10*, 2795−2799.
(30) Li, I. T. S.; Walker, G. C. *J. Am. Chem. Soc.* **2010**, *132*, 6530−6540.
(31) Fixman, M.; Kovac, J. *J. Chem. Phys.* **1973**, *58*, 1564−1568.
(32) Marko, J. F.; Siggia, J. F. *Macromolecules* **1995**, *28*, 8759−8770.
(33) Livadaru, L.; Netz, R. R.; Kreuzer, H. J. *Macromolecules* **2003**, *36*, 3732−3744.
(34) Serr, A.; Horinek, D.; Netz, R. R. *J. Am. Chem. Soc.* **2008**, *130*, 12408−12413.
(35) Hanke, F.; Serr, A.; Kreuzer, H. J. *Europhys. Lett.* **2010**, *92*, 53001.
(36) Germann, M. W.; Turner, T.; Allison, S. A. *J. Phys. Chem. A* **2007**, *111*, 1452−1455.